nature portfolio

https://doi.org/10.1038/s41558-021-01000-1

Supplementary information

Anthropogenic climate change has slowed global agricultural productivity growth

In the format provided by the authors and unedited

Supplementary Information for

Anthropogenic Climate Change Has Slowed Global Agricultural Productivity Growth

Ariel Ortiz-Bobea, Toby R. Ault, Carlos M. Carrillo, Robert G. Chambers, David B. Lobell

Correspondence to: ao332@cornell.edu

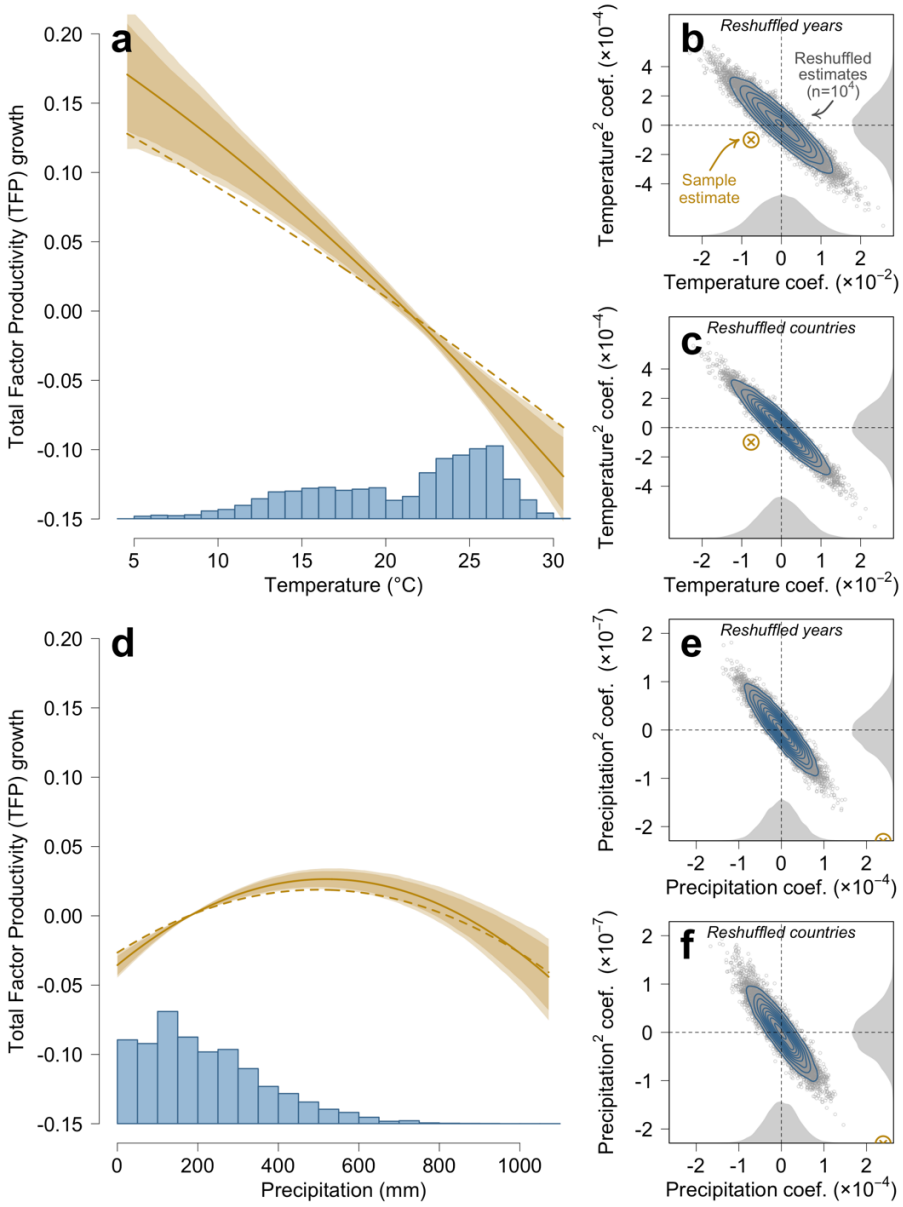

Supplementary Fig. 1: The response of agricultural output to weather. a. Response function of OUTPUT growth to changes in green-season average T. Response functions are centered vertically so that the exposure-weighted marginal effect is zero. The baseline response function for TFP, with all countries and years, is shown in dashed lines. The colored bands represent 90 and 95% confidence bands based on 500 year-by-region block bootstraps. The blue bars represent the country-level distribution of green-season average T over the sample period 1962-2015. The average green-season T is indicated for a select number of large countries. **b.** Panel shows the result of a placebo check whereby OUTPUT and weather data are randomly mismatched or reshuffled by years. The distribution represents the linear and quadratic T coefficients based on 10,000 reshuffled datasets. **c.** Same as previous panel but based on datasets reshuffled by country. **d.** Response function of changes in country-level OUTPUT to changes in green-season total P. **e.** Same as panel **b.** but for P coefficients. **f.** Same as panel **c** but for P coefficients.

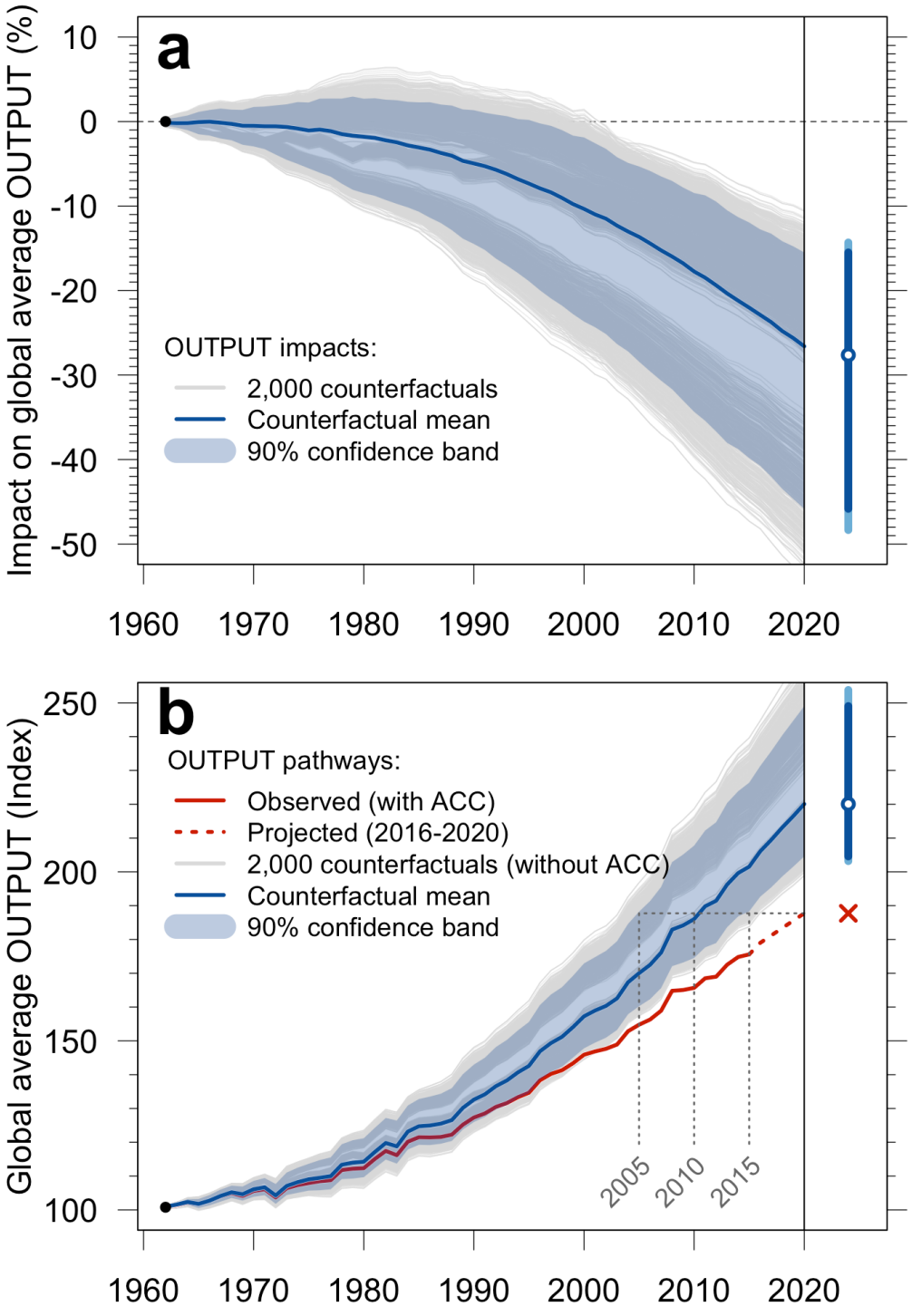

Supplementary Fig. 2. Global impact of anthropogenic climate change on output. a. 2,000 counterfactual paths ways combining statistical uncertainty and climate uncertainty. Blue line shows ensemble mean and the blue cone represents a 90% confidence band. The error bars on the right indicate 90 and 95% confidence intervals for the impact on 2020. **b.** Same results presented in levels relative to the observed (1962-2015) and projected (2016-2020) level of TFP (in red).

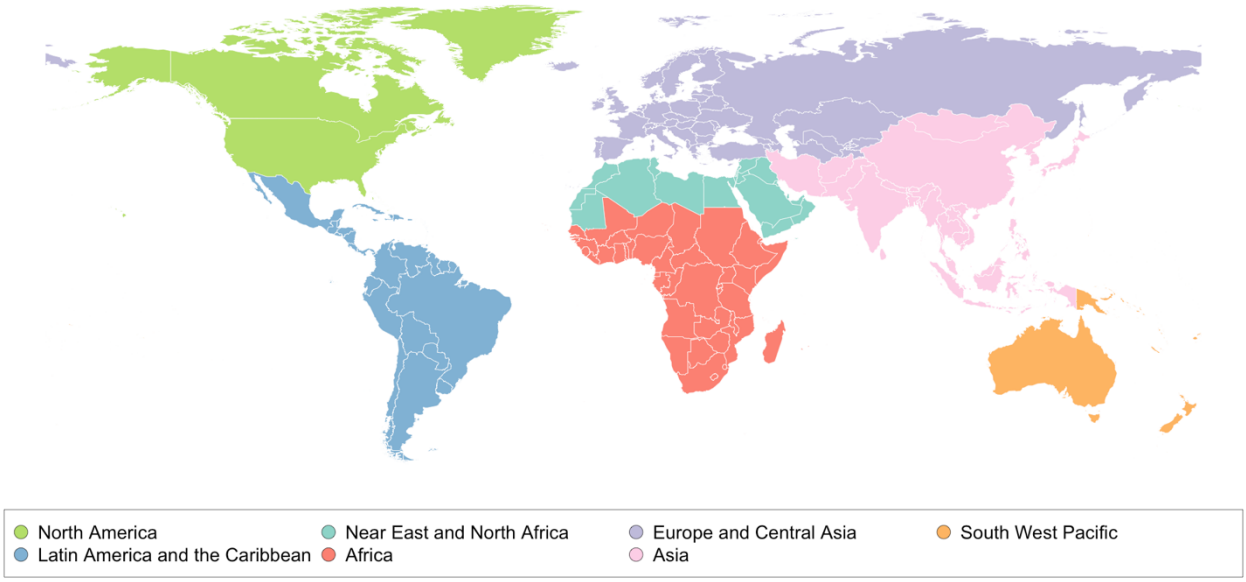

Supplementary Fig. 3. FAO regions used in the study.

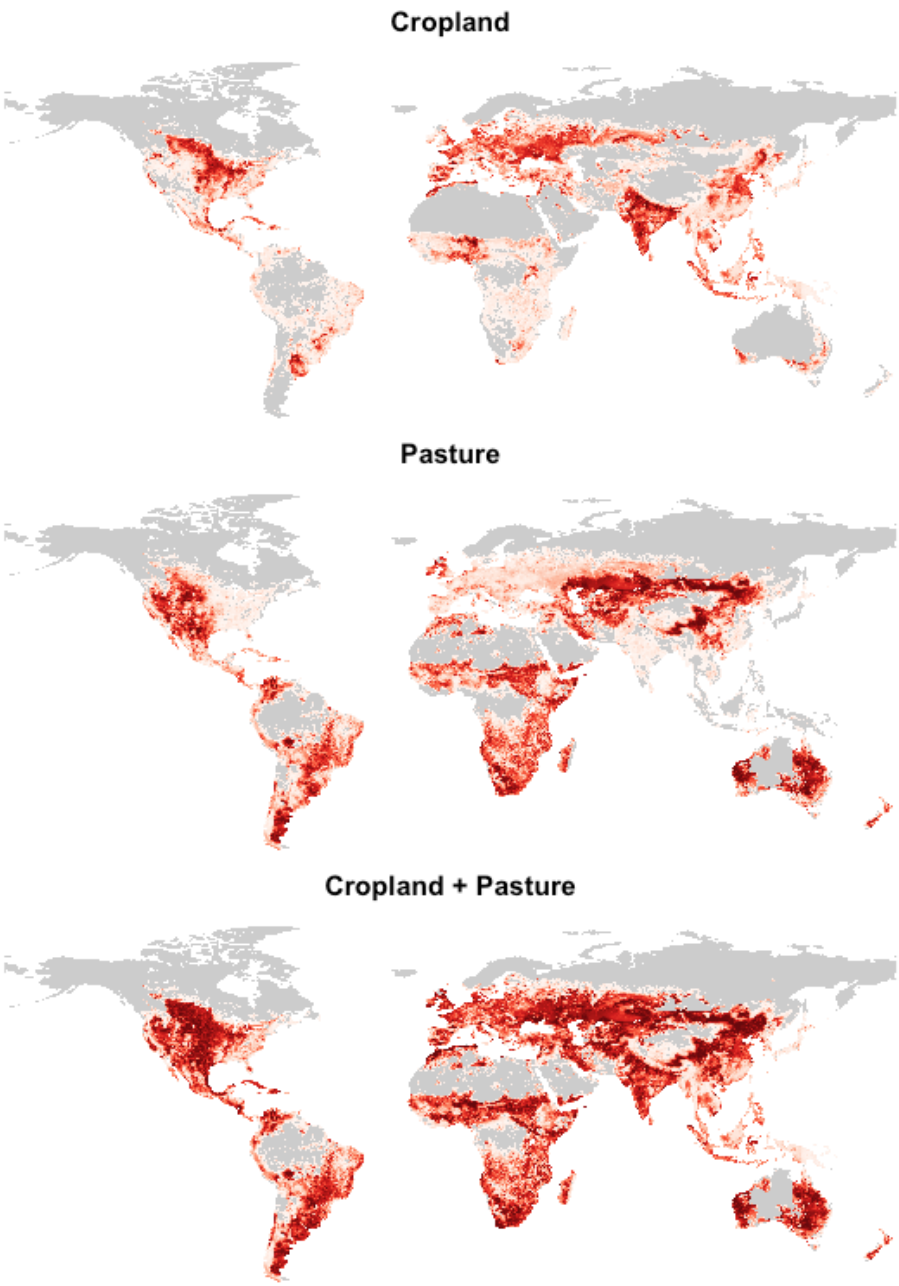

Supplementary Fig. 4. Land cover weights for aggregating gridded GMFD weather data to the country level.

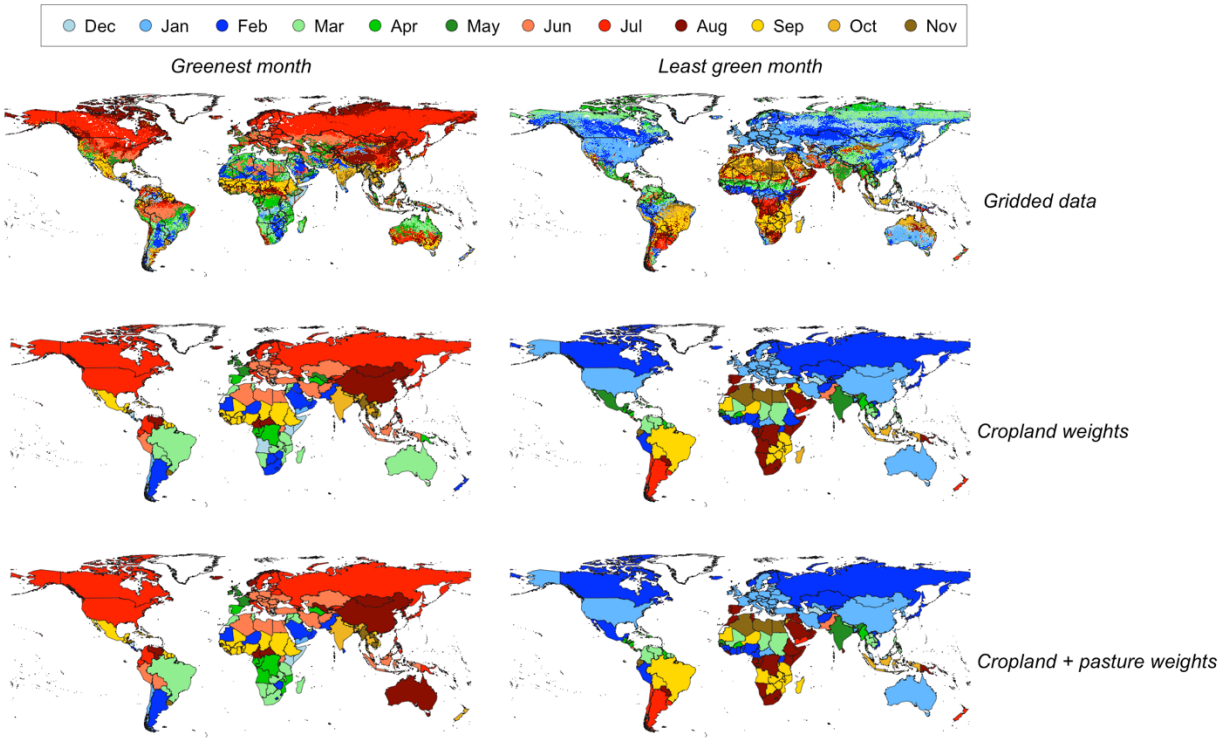

Supplementary Fig. 5. Month with highest and lowest value of NDVI. Native raster grid shown on the first row. The second and third indicate values aggregated to the country level based on cropland and cropland+pasture frequency weights, respectively.

Supplementary Table 1. Regression results for the baseline model.

	Coefficient	Std. Error (bootstrapped)	t-stat	P-value
ΔTavg	6.48×10^{-3}	4.87×10^{-3}	-1.33	0.184
ΔTavg squared	-4.75×10^{-5}	12.57×10^{-5}	-0.38	0.705
ΔPrecipitation	1.82×10^{-4}***	0.35×10^{-4}	5.19	2.1×10^{-7}
ΔPrecipitation squared	-1.82×10^{-7}***	0.41×10^{-9}	-4.45	8.5×10^{-6}
R^2	0.04			
N	9,255			

Notes: Signif. codes: 0 '***' 0.001 '**' 0.01 '*' 0.05 '.' 0.1 ' ' 1. Standard errors are obtained via a block bootstrap (R=500) where blocks correspond to year-FAO regions. Note that significance levels on individual coefficients are not very meaningful when variables are highly correlated, as in the case of Tavg and $Tavg^2$. A Wald test rejects the hypothesis that temperature coefficients are jointly equal to 0 ($P = 3.06 \times 10^{-5}$).

Supplementary Table 2. Test whether the sum of coefficients for lagged of weather variables differs from zero in the baseline model.

Number of lags of weather variables	Wald statistic	Degrees of freedom (number of parameter restrictions)	P-value
1	0.42	1	0.518
2	0.48	1	0.486
3	2.86	1	0.091
4	1.43	1	0.232
5	2.46	1	0.117
6	0.79	1	0.374
7	2.17	1	0.141
8	0.41	1	0.522
9	0.56	1	0.454
10	2.23	1	0.135

Supplementary Table 3. Cumulative impacts of ACC on regional agricultural TFP (1961-2020).

FAO Region	Mean (%)	Percentiles (%)			
		10%	90%	5%	95%
Africa	−34.0	−53.4	−10.0	−60.0	−4.0
Near East and North Africa	−30.0	−49.0	−13.0	−55.6	−9.6
Latin America and the Caribbean	−25.9	−45.5	−1.5	−53.6	7.2
Asia	−19.4	−37.4	−6.0	−43.5	−3.7
South West Pacific	−19.3	−39.6	11.5	−45.6	25.5
North America	−12.5	−36.3	7.0	−42.9	13.2
Europe and Central Asia	−7.1	−26.2	13.3	−34.2	18.3
Global	−17.3	−35.5	−4.0	−41.1	−1.4

Supplementary Table 4. List of General Circulation Models (GCMs) in CMIP6 used in the study.

#	GCM
1	BCC-CSM2-MR
2	CanESM5
3	CNRM-CM6-1
4	HadGEM3-GC31-LL
5	IPSL-CM6A-LR
6	MIROC6
7	MRI-ESM2-0